

Node Copying: A Random Graph Model for Effective Graph Sampling

Florence Regol^{1†}, Soumyasundar Pal^{1†}, Jianing Sun², Yingxue Zhang²,
Yanhui Geng², and Mark Coates¹

¹Dept. of Electrical and Computer Engineering, McGill University, Montreal, QC, Canada.

²Huawei Noah’s Ark Lab, Montreal Research Center, Montreal, QC, Canada.

Abstract

There has been an increased interest in applying machine learning techniques on relational structured-data based on an observed graph. Often, this graph is not fully representative of the true relationship amongst nodes. In these settings, building a generative model conditioned on the observed graph allows to take the graph uncertainty into account. Various existing techniques either rely on restrictive assumptions, fail to preserve topological properties within the samples or are prohibitively expensive for larger graphs. In this work, we introduce the node copying model for constructing a distribution over graphs. Sampling of a random graph is carried out by replacing each node’s neighbors by those of a randomly sampled similar node. The sampled graphs preserve key characteristics of the graph structure without explicitly targeting them. Additionally, sampling from this model is extremely simple and scales linearly with the nodes. We show the usefulness of the copying model in three tasks. First, in node classification, a Bayesian formulation based on node copying achieves higher accuracy in sparse data settings. Second, we employ our proposed model to mitigate the effect of adversarial attacks on the graph topology. Last, incorporation of the model in a recommendation system setting improves recall over *state-of-the-art* methods.

Keywords— Generative graph model, graph neural network, adversarial attack, recommender systems

1 Introduction

In graph related learning problems, models need to take into account relational structure. This additional information is encoded by a graph that represents data points as nodes and the relationships as edges. In practice, observed quantities are often noisy and the information used to construct a graph is no exception. The provided graph is likely to be incomplete and/or contain spurious edges. For some graph learning tasks, this error or incompleteness is explicitly stated. For example, in the recommendation system setting, the task is to infer unobserved links representing users’ preferences for items. In other cases, such as protein-protein interaction networks, graph uncertainty is implicit, arising because the graphs are constructed from noisy measurement data.

In these cases, we can view the graph as a random quantity. The modelling of random graphs as realisations of statistical models has been widely studied in network analysis [1]. Parametric random graph models have been used extensively to study complex systems and perform inference [2, 3, 4]. Parameters are usually estimated based on the observed graph. However, these models often fail to capture the structural properties of real-world networks and as a result, are not suitable as generative

[†]These authors contributed equally to this work.

Corresponding author: Florence Regol (email address: florence.robert-regol@mail.mcgill.ca)

models. In addition, inference of parameters can be prohibitively expensive for large scale networks, and many parametric models cannot take into account node or edge attributes.

Recent interest in generative models for graph learning has resulted in auto-encoder based formulations [5, 6]. There has also been an effort to combine the strengths of parametric random graph models and machine learning approaches [7]. In these models, the probability of the presence of an edge is related to the node embeddings of the incident nodes. Although the auto-encoder solutions excel in their targeted objective of link prediction, they fail to generate representative samples [8]. In [8, 9], application of generative adversarial networks (GANs) is considered for graph generative models. [8] shows that the GAN generated graphs do not deviate from the observed graph in terms of structural properties. These approaches are promising but the required training time can be prohibitive for graphs of even a moderate size.

The main contribution of this paper is to introduce a novel generative model for graphs for the case when we have access to a single observed graph. The generative model is designed to allow the sampling of multiple graphs that can be used as an ensemble to improve performance in graph-based learning tasks. We call the approach “node copying”. Based on a similarity metric between nodes, the node copying model generates random graph realizations by replacing the edges of a node in the observed graph with those of a randomly chosen similar node. The assumption made by this model is that *similar* nodes should have *similar* neighborhoods. The meaning of ‘similar’ varies depending on how the model is employed in a learning task and has to be defined according to the application setting. Most graph learning algorithms rely on and exploit the property of homophily, which implies that nodes with similar characteristics are more likely to be connected to one another [10]. The proposed node copying model preserves this homophily (one similar neighbourhood is swapped for another similar neighbourhood). The advantage is that the generative model permits sampling of an ensemble of graphs that can be used to improve the performance of learning algorithms, as illustrated in later sections of the paper.

By construction, each sampled graph possesses the same set of nodes as the observed graph and the identities of the nodes are retained throughout the sampling procedure. The identity of a node is specified by a label and/or a set of node features; hence, each node preserves its own features or labels (if available) in the sampled graphs. The proposed model is simple and the computational overhead is minimal. Despite its simplicity, we show that incorporating such a model can be beneficial in a range of graph-based learning tasks. The model is flexible in the sense that the choice of the similarity metric is adapted to the end-to-end learning goal. It can be combined with *state-of-the-art* methods to provide an improvement in performance. In summary, the proposed model: 1) *generates useful samples* which improve the performance in graph-based machine learning tasks and retain important structural properties; 2) *is flexible* so that it is applicable to various tasks (e.g., the bipartite graphs in recommendation systems are drastically different from the community structured graphs considered in node classification); and 3) *is fast* both for model construction and random sample generation.

Extensive experiments demonstrate the effectiveness of our model for three different graph learning tasks. We show that the incorporation of the model in a Bayesian framework for node classification leads to improved performance over *state-of-the-art* methods for the scarce data scenario. The model has much lower computational complexity compared to other Bayesian alternatives. In the face of adversarial attacks, a node copying based strategy significantly mitigates the effect of the corruption. Lastly, the use of the node copying model in a personalized recommender system leads to improvement over a *state-of-the-art* graph-based method. Preliminary results for application of the node copying model in semi-supervised node classification and in defense against adversarial attacks were published in [11] and [12] respectively. In this paper, we add theoretical results to shed light on the statistical properties of the sampled graphs in special cases, conduct thorough experimentation to examine the similarity of the sampled graphs to the observed graph, show the effectiveness of the proposed approach in a data-scarce classification problem and against diverse adversarial attacks, and extend the application of the copying model to the recommendation setting.

2 Related work

Parametric random graph models: There is a rich history of research and development of parametric models of random graphs. These models have been designed to generate graphs exhibiting specific characteristics and their theoretical properties have been studied in depth. They can yield samples representative of an observed graph provided that the model is capable of representing the particular graph structure and parameter inference is successful. The Barabasi-Albert model [2], exponential random graphs [3], exchangeable random graph models [13], and the large family of stochastic block models (SBMs) [14], including mixed-membership SBMs [4], degree-corrected SBMs [15], and overlapping SBMs [16, 17]), fall into this category. Configuration model [18, 19] variants preserve the degree sequence of a graph while changing the connectivity pattern in the random samples. [20] provides a recent survey of various random graph models. A major drawback of these models is that they impose relatively strict structural assumptions in order to maintain tractability. As a result, they often cannot model characteristics like large clustering coefficients [21], small world connectivity and exponential degree distributions [22], observed in many real-world networks. Additionally, most cannot readily take into account node or edge attribute information, and high-dimensional parameter inference can be prohibitively computationally expensive for larger graphs.

Learning-based models: Other generative graph models have emerged from the machine learning community, incorporating an auto-encoder structure. The models are commonly trained to accurately predict the links in the graph, and as a result, tend to fail to reproduce global structural properties of the observed graph. [5] introduces a variational auto-encoder based model parameterized by a graph convolutional network (GCN) to learn node embeddings. The link probabilities are derived from the dot product of the obtained node embeddings. [23] adopts a similar approach, but employs adversarial regularization to learn more robust embeddings. Both of these models exhibit impressive clustering of node embeddings. [24] adds a message passing component to the decoder that is based on intermediately learned graphs. This leads to improved representations and better link prediction. [7] combines the strengths of the parametric models and the graph-based learning methods, proposing the DGLFRM model, which aims to retain the interpretability of the overlapping SBM (OSBM) paired with the flexibility of the graph auto-encoder. The incorporation of the OSBM improves the ability of the model to capture block-based community structure.

An alternative approach is to use generative adversarial networks (GANs) as the basis for graph models. [9] models edge probability through an adversarial framework in the GraphGAN model. The NetGAN model represents the graph as a distribution on random walks [8]. Compared to auto-encoder based methods, the GAN based methods seem more capable of capturing the structural characteristics of an observed graph. The major disadvantage is that the models are extremely computationally demanding to train and the success of the training can be sensitive to the choice of hyperparameters.

Our focus in this paper is on learning a graph model based on a single observed graph. By contrast, there is a growing body of work that focuses on learning graph models that can reproduce graphs that have characteristics similar to a dataset of multiple training graphs. These approaches can preserve important structural attributes of the graph(s) in the dataset, but the sampled graphs do not retain node identity information. They cannot be applied in the node- and edge-oriented learning tasks we focus on. In this category, there have been variational auto-encoder approaches [25, 26], GAN-based approaches [27], models based on iterative generation [28], and auto-regressive models [29, 30].

3 Node copying model

We propose to build a random graph model by introducing random perturbations to an initial observed graph \mathcal{G}_{obs} . Our aim is to generate graphs \mathcal{G} that are close to \mathcal{G}_{obs} in some structural sense, while preserving any metadata associated with a node’s identity (e.g., node features, labels). Here, we consider that $\mathcal{G}_{obs} = \{\mathcal{V}_{obs}, \mathcal{E}_{obs}\}$ is a directed graph (the extension to the undirected case is straightforward and will be explained at the end of this section). \mathcal{V}_{obs} denotes the set of N nodes and \mathcal{E}_{obs} is the set of directed edges of the form $(i, j, A_{\mathcal{G}_{obs},ij})$ which indicates that there is a directed edge from node i to node j with edge weight encoded in the adjacency matrix $A_{\mathcal{G}_{obs}} \in \mathbb{R}_+^{N \times N}$. For the sampled

graph $\mathcal{G} = \{\mathcal{V}, \mathcal{E}\}$, we have the same set of vertices as \mathcal{G}_{obs} i.e. $\mathcal{V} = \mathcal{V}_{obs}$ but the connectivity pattern is different i.e. $\mathcal{E} \neq \mathcal{E}_{obs}$.

To that end, we introduce a discrete perturbation random vector $\zeta \in S_{\zeta}^N$, whose entries can have values from a finite or countably infinite set S_{ζ} and define a mapping $T : \mathbb{R}_+^{N \times N} \times S_{\zeta}^N \rightarrow \mathbb{R}_+^{N \times N}$ whose output is an adjacency matrix $A_{\mathcal{G}} \in \mathbb{R}_+^{N \times N}$ of the same dimension as the observed adjacency matrix $A_{\mathcal{G}_{obs}} \in \mathbb{R}_+^{N \times N}$, based on the inputs $A_{\mathcal{G}_{obs}}$ and ζ . We require \mathcal{G} to have the same set of nodes as \mathcal{G}_{obs} ; hence, \mathcal{G} is fully characterized by $A_{\mathcal{G}}$.

The mapping is not necessarily one-to-one, i.e., multiple ζ s can generate the same graph \mathcal{G} . The probability of generating a specific graph \mathcal{G} is then specified by defining a probability distribution for ζ . We model the distribution of ζ to be conditioned on \mathcal{G}_{obs} and possible additional information \mathcal{D} (e.g. node/edge labels or features). We therefore obtain the following conditional probability:

$$p(\mathcal{G}|\mathcal{G}_{obs}, \mathcal{D}) = \sum_{\zeta} p(\zeta|\mathcal{G}_{obs}, \mathcal{D}) \mathbb{1}[T(A_{\mathcal{G}_{obs}}, \zeta) = A_{\mathcal{G}}], \quad (1)$$

where $\mathbb{1}[\cdot]$ denotes the indicator function, which takes the value one if $T(A_{\mathcal{G}_{obs}}, \zeta) = A_{\mathcal{G}}$ and is zero otherwise. This is the foundation of our proposed copying model. We propose a ‘node copying’ mechanism to implement the mapping T . The intuition for the node copying mechanism is as follows. Suppose two nodes, i and j , are ‘similar’, where ‘similarity’ depends on the context or application setting. It may be defined in terms of node attributes, node labels, structural properties, or a combination of all of these. Then we conjecture that similar nodes also have similar neighbourhoods. For example, suppose both nodes have the same label. Then, in a homophilic graph, most of their neighbours also have the same label, and the neighbourhoods are thus similar. If we replace node i ’s neighbourhood with that of node j (the copy operation), then we obtain a new graph, but the homophilic nature of the graph is preserved.

To make our random graph model concrete, we need to specify 1) the mapping T with the nature of ζ and 2) the conditional distribution $p(\zeta|\mathcal{G}_{obs}, \mathcal{D})$.

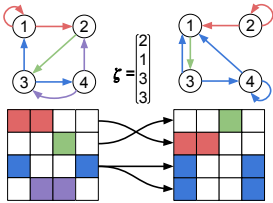


Figure 1: Application of the node copying T on observed graph \mathcal{G}_{obs} (left-side) for a given ζ to obtain \mathcal{G} (right-side).

1) *Mapping $T(\cdot, \cdot)$ and random vector ζ* : We construct a **node copying mapping** T that replaces the neighborhood of a node i by that of another node given by the i -th entry of the vector $\zeta = [\zeta^1, \zeta^2, \dots, \zeta^N]^T \in \{1, 2, \dots, N\}^N$. ζ^i is referred to as the *replacement node* of node i . An explicit expression for T can be provided using a selection matrix $C_{\zeta} \in \{0, 1\}^{N \times N}$, where $C_{\zeta}[i, j] = 1$ if $j = \zeta^i$ and 0 otherwise. Then $T(A_{\mathcal{G}_{obs}}, \zeta) = C_{\zeta} A_{\mathcal{G}_{obs}} = A_{\mathcal{G}}$. Figure 1 depicts the application of the mapping T on example \mathcal{G}_{obs} and ζ to obtain a graph \mathcal{G} .

2) *Distribution $p(\zeta|\mathcal{G}_{obs}, \mathcal{D})$* : The distribution for ζ should encode the notion of node similarity, and is there-

fore task dependant. The entries in ζ are assumed to be mutually independent to facilitate inference: $p(\zeta|\mathcal{G}_{obs}, \mathcal{D}) = \prod_{j=1}^N p(\zeta^j|\mathcal{G}_{obs}, \mathcal{D})$. We provide examples of candidate probability distributions in later sections. One approach is to train a node embedding algorithm to learn $\{\mathbf{e}_i\}_{i=1:N} = f_{\Theta}(\mathcal{G}_{obs}, \mathcal{D})$, where \mathbf{e}_i denotes the representation of node i . The probability $p(\zeta^j = i|\mathcal{G}_{obs}, \mathcal{D}) \propto \text{sim}(\mathbf{e}_j, \mathbf{e}_i)$ to promote frequent copying between nodes if they are ‘similar’, for some function $\text{sim}(\cdot, \cdot)$, which measures similarity between two nodes.

This completes the description of our proposed model. Sampling a graph \mathcal{G} from the node copying model involves sampling each element of ζ independently according to $p(\zeta^j|\mathcal{G}_{obs}, \mathcal{D})$. Once ζ is constructed, we replace the out-edges of the i -th node in the observed graph \mathcal{G}_{obs} by those of the ζ^i -th node. In general, we construct the distribution $p(\zeta^j|\mathcal{G}_{obs}, \mathcal{D})$ so that it is simple to sample from. We thus avoid any need to use MCMC or importance sampling for drawing the sampled graphs. For using this model to sample undirected graphs when \mathcal{G}_{obs} is undirected, we apply the following procedure. We treat \mathcal{G}_{obs} as a directed graph and use the node copying model to sample a directed graph \mathcal{G}' . Then, we change each directed edge to an undirected edge to obtain an undirected graph \mathcal{G} by setting $A_{\mathcal{G}, ij} = \max(A_{\mathcal{G}', ij}, A_{\mathcal{G}', ji})$.

Remark 1. *Since the model is defined in terms of perturbations of the observed graph \mathcal{G}_{obs} , the utility of the proposed graph model hinges on \mathcal{G}_{obs} being a meaningful starting point for inference. In some cases, even if no graph is directly available for a problem, we can learn relationships between entities and construct \mathcal{G}_{obs} from the available data. Computationally efficient techniques for such graph construction are reported in [31, 32]. In some cases, the computational requirements can still be considerable.*

4 Analysis and comparison of sampled graphs

In order to gain insight into the properties of the random graphs drawn from the node copying model, we evaluate several properties of the samples and compare with other generative methods and the observed graph, for four datasets.

Node Embedding Baselines: We compare with various graph-based auto-encoder models, which are trained to optimize an unsupervised variational objective for a link prediction task. Specifically we compare with the Variational Graph Auto-Encoder (VGAE) [5], GRAPHITE [24] and DGLFRM-B [7] algorithms. In each algorithm, the probability of an edge between any two nodes depends on the learned embeddings. The probability of an edge between nodes i and j from a specific model is denoted as p_{ij}^{model} . Instead of their originally proposed use for link prediction, we wish to evaluate these models as generative models. Hence, we train the models using the entire graph and estimate $\{p_{ij}^{model}\}_{1 \leq i \leq j \leq N}$. We refer to these probabilities as ‘raw’ probabilities and sample graphs according to them. In practice, this results in dense sampled graphs where the edge densities in the sampled graphs are multiple orders-of-magnitude higher than the density of the observed graph \mathcal{G}_{obs} . As a result, many of the statistics of the sampled graphs are not comparable with those of \mathcal{G}_{obs} . In order to sample more realistic graphs, we employ logistic regression based calibration. We fit a model $p_{ij}^{cal} = p(A_{obs,ij} = 1 | p_{ij}^{model}) = \sigma(\alpha p_{ij}^{model} + \beta)$ (where $\sigma(\cdot)$ denotes the sigmoid function) to learn (α, β) and use the predicted probabilities for sampling graphs. Even after calibration the densities of the sampled graphs are still too high, so we explicitly re-scale the calibrated probabilities such that the sampled graphs in expectation have the same number of edges $|\mathcal{E}_{obs}|$ as \mathcal{G}_{obs} : $p_{ij}^{cc} = \frac{|\mathcal{E}_{obs}| p_{ij}^{cal}}{\sum_{i=1}^N \sum_{j=1}^N p_{ij}^{cal}}$.

We call this procedure ‘calibration and correction’ (cc).

Node copying: Since the baselines are unsupervised techniques, for a fair comparison we refrain from using node labels for the node copying model. Instead, we sample replacement nodes according to the distances between learned embeddings. The selected datasets are used as benchmark for node classification task and are expected to exhibit some homophilic property, which suggests that nodes with the same label are clustered together and share similar features. This indicates that it is sensible to construct a similarity metric using node embeddings that are derived from both topological and feature information. Specifically, for any node, we sample the replacement node uniformly from the K -nearest neighbors according to the Euclidean distance between embeddings.

Experiment: The qualitative similarity of two graphs can be measured in multiple ways. To obtain an insight into which method can generate graphs that are the closest to an original graph, we report various graph statistics on the sampled graphs and compare them to the statistics of the observed graphs for Cora, Polblogs, Bitcoin, and Amazon-photo datasets (homophilic graphs, used extensively for node classification) in Table 1. Details of all datasets used in this paper are included in A. For uniformity, the directed graph of Bitcoin has been made undirected by casting every in/out edge as an undirected edge.

Metrics: For a graph \mathcal{G} , $d(v)$ is the degree of node v and c_v denotes the class label of node v . We report the average and minimum degree, the proportion of cross-community edges: $\frac{1}{|\mathcal{E}|} \sum_{(i,j) \in \mathcal{E}} \mathbb{1}[c_i \neq c_j]$, the proportion of claws (‘Y’ structure): $\frac{1}{\binom{|\mathcal{E}|}{3}} \sum_{v \in \mathcal{V}} \binom{d(v)}{3}$ and the relative entropy of the edge distribution: $\frac{1}{\log N} \sum_{v \in \mathcal{V}} \frac{-d(v)}{|\mathcal{E}|} \log \left(\frac{d(v)}{|\mathcal{E}|} \right)$. By reporting various summary graph statistics, we can have a broad picture of the properties of the generated graphs.

In each case, 10 random trials of the model training are conducted and 10 random graphs are sampled based on each trial. The results are thus averaged over $10 \times 10 = 100$ sampled graphs. We

Table 1: Average statistics of 100 sampled graphs. Bolded entries indicate the closest values to the observed value. N/A indicates entries that were not reported due to processing limitations.

| | Avg. degree | Max. degree | Cross com. % | Claws % ($\times 10^{-4}$) | Edge dist. ent. (%) | Avg. degree | Max. degree | Cross com. % | Claws % ($\times 10^{-4}$) | Edge dist. ent. (%) |
|----------------------|--------------------|--------------------|--------------|------------------------------|---------------------|---------------------|--------------------------------------|--------------|------------------------------|---------------------|
| Cora | | | | | | Polblogs | | | | |
| Observed | 3.89 | 168 | 19.6 | 6.34 | 95.6 | 27.4 | 351 | 9.42 | 10.1 | 90.3 |
| GRAPHITE (cc) | 3.9 | 24 | 34.4 | 0.43 | 96 | 27.3 | 64 | 18.1 | 0.91 | 98.9 |
| raw | 1.3×10^3 | 1.4×10^3 | 77.6 | 0.18 | 100 | 614 | 712 | 39.2 | 0.67 | 100 |
| calibrated | 105 | 519 | 34.5 | 0.44 | 97.7 | 256 | 530 | 18.1 | 0.91 | 99.2 |
| GVAE (cc) | 3.9 | 22.1 | 37 | 0.302 | 96.2 | 27.3 | 64.1 | 18.2 | 0.918 | 98.9 |
| raw | 1.34×10^3 | 1.44×10^3 | 77.7 | 0.136 | 100 | 614 | 714 | 39.4 | 0.673 | 100 |
| calibrated | 125 | 587 | 37 | 0.309 | 97.9 | 255 | 533 | 18.2 | 0.918 | 99.1 |
| DGLFRM-B (cc) | 3.9 | 14.9 | 38.8 | 0.169 | 97.8 | 27.3 | 58.8 | 18.1 | 0.874 | 99 |
| COPYING K=5 | 3.5 | 105 | 18.4 | 3.2 | 96.9 | 26 | 311 | 8.94 | 8.61 | 90.6 |
| COPYING K=10 | 3.3 | 63.9 | 20.4 | 1.22 | 97.4 | 25.5 | 290 | 8.83 | 7.72 | 90.8 |
| COPYING K=15 | 3.2 | 58.1 | 22 | 1.1 | 97.5 | 25.2 | 274 | 8.72 | 7.33 | 90.9 |
| Bitcoins | | | | | | Amazon-photo | | | | |
| Observed | 2.08 | 53 | 27.1 | 240 | 92.3 | 31.8 | 1.43×10^3 | 17.3 | 0.75 | 94.2 |
| GRAPHITE (cc) | 2.09 | 9.21 | 23.8 | 6.22 | 94.7 | 31.8 | 87.2 | 81.3 | 0.02 | 99.3 |
| raw | 250 | 311 | 37.6 | 4.97 | 99.8 | 4.4×10^3 | 6.0×10^3 | 83.1 | 0.02 | 100 |
| calibrated | 84.8 | 219 | 23.8 | 9.48 | 99.1 | 2.7×10^3 | 6.4×10^3 | 81.3 | 0.02 | 99.4 |
| GVAE (cc) | 2.09 | 9.18 | 22.2 | 6.24 | 94.8 | 31.8 | 71.7 | 80.2 | 0.0212 | 99.5 |
| raw | 236 | 285 | 37.1 | 4.62 | 99.9 | 5.41×10^3 | 6.24×10^3 | 82.4 | 0.0226 | 100 |
| calibrated | 72.4 | 198 | 22.2 | 6.96 | 99.1 | 2.95×10^3 | 4.84×10^3 | 80.2 | 0.0228 | 99.7 |
| DGLFRM-B (cc) | 235 | 291 | 36.9 | 4.59 | 99.9 | N/A | N/A | N/A | N/A | N/A |
| COPYING K=5 | 1.8 | 34.9 | 23.6 | 125 | 95.3 | 31.5 | 1.04×10^3 | 41.5 | 0.532 | 94.7 |
| COPYING K=10 | 1.73 | 28.3 | 23 | 89.9 | 96.0 | 31.1 | 1.05×10^3 | 47.2 | 0.502 | 94.9 |
| COPYING K=15 | 1.68 | 21 | 22.6 | 50.3 | 96.7 | 31 | 1.03×10^3 | 50.6 | 0.502 | 94.9 |

observe that without the ‘calibration and correction’, the baseline node embedding algorithms fail to generate representative graphs as the characteristics of the sampled graphs show large deviation from those of the observed graph. In particular, in ‘raw’ versions, we obtain graph samples which are significantly denser, have higher proportion of cross-community links, have lower proportion of claws, and possess a flatter degree distribution compared to the observed graph. This shows that learning node embeddings while targeting a link prediction task does not necessarily result in a good generative model.

‘Calibration’ reduces this effect and leads to sparser graphs with better cross-community structure. After the explicit ‘correction’, the average degree of the sampled graphs is the same as that of the observed graph. However, the degree distribution still does not match with that of the observed graph, as evident from the maximum degree, as well as the relative entropy of the edge distribution. Moreover, the sample graphs have a much lower proportion of claws. This is not unexpected, because any model which is based on independence of the links cannot model such local structural dependencies observed in real world graphs. On the other hand, the samples from the proposed node copying model show a much better agreement with the observed graph in terms of all the statistics we consider. In particular, a much lower proportion of cross-community links in the graph samples of the copying model provides a rationale for its efficacy when the model is adopted for a node classification task. Overall, these tendencies can be observed when sampling is performed using a different number of nearest neighbors for the sampling distribution ($K = 5, 10, 15$). In this experiment, sampling from the $K = 5$ nearest neighbors seems to be the best choice.

Connections to other random graph models: We further support this notion that the copying model preserves the structure of the observed graph with theoretical results. We show that if the observed graph itself is a sample from some parametric random graph model, then suitable copying procedures can ensure that the sampled graphs have the same marginal distribution. We prove this result for two popular random graph models, namely for the Stochastic Block Model in Theorem 4.1 and for the Erdős-Rényi family in Theorem 4.2.

Theorem 4.1. *Let \mathcal{G}_{obs} be a sample of a Stochastic Block Model (SBM) with N nodes and K communities and symmetric conditional probability matrix $\beta \in \mathbb{R}^{K \times K}$. We use a node copying procedure*

between nodes of the same label, i.e., a node j cannot be copied in place of node i , if the labels $c_i \neq c_j$. Then any sampled graph \mathcal{G}_{sa} is marginally another realization from the same SBM.

Proof. For \mathcal{G}_{obs} , we have $p(A_{ij}^{obs} = 1 | c_i, c_j) = \beta_{c_i, c_j}$. Now, based on the copying strategy above, the probability of observing an edge (i, j) in \mathcal{G}_{sa} is given by:

$$\begin{aligned} p(A_{ij}^{sa} = 1 | c_i, c_j) &= \sum_{v=1}^N p(A_{vj}^{obs} = 1 | c_i, c_j, \zeta^i = v) p(\zeta^i = v | c_i, c_v), \\ &= \sum_{v: c_i = c_v} p(A_{vj}^{obs} = 1 | c_i, c_j, \zeta^i = v) p(\zeta^i = v | c_i, c_v) \quad (\text{since } p(\zeta^i = v | c_i \neq c_v) = 0), \\ &= \beta_{c_i, c_j} = p(A_{ij}^{obs} = 1 | c_i, c_j), \end{aligned} \quad (2)$$

since, $p(A_{vj}^{obs} = 1 | c_i, c_j, \zeta^i = v) = \beta_{c_i, c_j} = p(A_{ij}^{obs} = 1 | c_i, c_j)$ for all $\{v : c_i = c_v\}$ and $\sum_{v: c_i = c_v} p(\zeta^i = v | c_i, c_v) = 1$. This is reliant on only copying within the same community, as $p(\zeta^i = v | c_i \neq c_v) = 0$. Next we consider the joint distribution of two edges, i.e. $p(A_{i_1 j_1}^{sa} = 1, A_{i_2 j_2}^{sa} = 1 | c_{i_1}, c_{i_2}, c_{j_1}, c_{j_2})$. We need to consider the following two cases:

Case 1: $i_1 \neq i_2$

$$\begin{aligned} &p(A_{i_1 j_1}^{sa} = 1, A_{i_2 j_2}^{sa} = 1 | c_{i_1}, c_{i_2}, c_{j_1}, c_{j_2}) \\ &= \sum_{v=1}^N \sum_{u=1}^N p(\zeta^{i_1} = v, \zeta^{i_2} = u | c_{i_1}, c_{i_2}) p(A_{v j_1}^{obs} = 1, A_{u j_2}^{obs} = 1 | c_{i_1}, c_{i_2}, c_{j_1}, c_{j_2}, \zeta^{i_1} = v, \zeta^{i_2} = u), \\ &= \sum_{\substack{v: \\ c_{i_1} = c_v}} \sum_{\substack{u: \\ c_{i_2} = c_u}} p(\zeta^{i_1} = v, | c_{i_1}) p(\zeta^{i_2} = u, | c_{i_2}) p(A_{v j_1}^{obs} = 1 | c_{i_1}, c_{j_1}, \zeta^{i_1} = v) p(A_{u j_2}^{obs} = 1 | c_{i_2}, c_{j_2}, \zeta^{i_2} = u), \\ &= \beta_{c_{i_1} c_{j_1}} \beta_{c_{i_2} c_{j_2}} = p(A_{i_1 j_1}^{obs} = 1, A_{i_2 j_2}^{obs} = 1 | c_{i_1}, c_{i_2}, c_{j_1}, c_{j_2}). \end{aligned} \quad (3)$$

Case 2: $i_1 = i_2$

$$\begin{aligned} &p(A_{i_1 j_1}^{sa} = 1, A_{i_2 j_2}^{sa} = 1 | c_{i_1} = c_{i_2}, c_{j_1}, c_{j_2}) \\ &= \sum_{v=1}^N p(\zeta^{i_1} = v | c_{i_1}) p(A_{v j_1}^{obs} = 1, A_{v j_2}^{obs} = 1 | c_{i_1} = c_{i_2}, c_{j_1}, c_{j_2}, \zeta^{i_1} = v), \\ &= \sum_{v: c_{i_1} = c_v} p(\zeta^{i_1} = v, | c_{i_1}) p(A_{v j_1}^{obs} = 1 | c_{i_1}, c_{j_1}, \zeta^{i_1} = v) p(A_{v j_2}^{obs} = 1 | c_{i_1}, c_{j_2}, \zeta^{i_1} = v), \\ &= \beta_{c_{i_1} c_{j_1}} \beta_{c_{i_1} c_{j_2}} = p(A_{i_1 j_1}^{obs} = 1, A_{i_1 j_2}^{obs} = 1 | c_{i_1} = c_{i_2}, c_{j_1}, c_{j_2}). \end{aligned} \quad (4)$$

Here, the joint distribution of ζ factorizes because of the independence of ζ^i 's. The joint conditional edge probability in \mathcal{G}_{obs} is the product of individual conditional edge probabilities as \mathcal{G}_{obs} is sampled from a SBM. Similarly, if we consider any arbitrary subset of the edges in \mathcal{G}_{sa} , we can show that the joint distribution is mutually independent over the edges and is the same as that of \mathcal{G}_{obs} . This proves the theorem. \square

Theorem 4.2. *If \mathcal{G}_{obs} is a sample of an Erdős-Rényi model with N nodes and connection probability $\theta \in [0, 1]$, then for any arbitrary distribution of ζ , \mathcal{G}_{sa} is also a sample from the same model.*

Proof. For \mathcal{G}_{obs} , we have $p(A_{ij}^{obs} = 1 | \theta) = \theta$. Now, based on any arbitrary copying strategy, we have

$$\begin{aligned} p(A_{ij}^{sa} = 1 | \theta) &= \sum_{k=1}^N p(\zeta^i = k | \theta) p(A_{kj}^{obs} = 1 | \theta, \zeta^i = k), \\ &= \theta = p(A_{ij}^{obs} = 1 | \theta), \end{aligned} \quad (5)$$

since $p(A_{kj}^{obs} = 1 | \theta, \zeta^i = k) = p(A_{ij}^{obs} = 1 | \theta) = \theta$ for $1 \leq k \leq N$ and $\sum_{k=1}^N p(\zeta^i = k | \theta) = 1$. Similarly, if we consider any arbitrary subset of the edges in \mathcal{G}_{sa} , we can show that the joint distribution is mutually independent over the edges and is the same as that of \mathcal{G}_{obs} . This proves the theorem. \square

Although generating samples that preserve graph structure can be useful, it is not the main purpose of our model. In the following three sections, we explain how this model can be applied in node classification, in protection against adversarial attack and in a recommendation system.

5 Application – Node copying for semi-supervised node classification

The node classification algorithms that we consider rely heavily on the homophily of the graph structure in predicting node labels. Nodes of the same label tend to be connected together more often than the nodes of different labels. If we define a notion of similarity which is based on the node labels, a node copying model can sample graphs which preserve the homophily property (see Theorem 4.1). Those graph samples can then be integrated in a Bayesian framework to make better prediction.

Problem Setting: In the task of semi-supervised node classification, apart from the observed graph \mathcal{G}_{obs} , we have access to node features \mathbf{X} and the labels in the training set $\mathbf{Y}_{\mathcal{L}}$. So, $\mathcal{D} = (\mathbf{X}, \mathbf{Y}_{\mathcal{L}})$. The goal is to infer the labels of the remaining nodes $\bar{\mathcal{L}} = \mathcal{V} \setminus \mathcal{L}$.

Bayesian GCNs - Background and Extension: A Bayesian framework for GCNs [33] (BGCN) views the graph \mathcal{G} and the GCN weights \mathbf{W} as random quantities and performs prediction by computing an expectation with respect to the posterior distribution. In [33], \mathcal{G}_{obs} is viewed as a sample realization from a *parametric* random graph model; the goal is the posterior inference of $p(\mathcal{G}|\mathcal{G}_{obs})$ marginalizing with respect to the random graph parameters. However, this approach ignores any possible dependence of the graph \mathcal{G} on the features \mathbf{X} and the labels $\mathbf{Y}_{\mathcal{L}}$ [34]. Although subsequent works address this issue, they either use variational approximation [35] of the posterior, or rely on *maximum a posteriori* (MAP) estimation [36]. Neither approach attempts to generate graph samples from the actual posterior.

We propose a modified version of the BGCN. In the proposed BGCN, the conditional distribution of the graph \mathcal{G} is represented as $p(\mathcal{G}|\mathcal{G}_{obs}, \mathbf{X}, \mathbf{Y}_{\mathcal{L}})$. This graph distribution can incorporate the information provided by the features \mathbf{X} and the training labels $\mathbf{Y}_{\mathcal{L}}$. In the classification task, the posterior is defined over the GCN weights \mathbf{W} . As in [37], we model the prior $p(\mathbf{W}) = \mathcal{N}(\mathbf{W}; \mathbf{0}, \mathbf{I})$. The likelihood $p(\mathbf{Y}_{\mathcal{L}}|\mathbf{X}, \mathcal{G}, \mathbf{W})$ is modelled using a K -dimensional categorical distribution by applying softmax function at the last layer of the Bayesian GCN over the graph \mathcal{G} . The posterior distribution of \mathbf{W} can be written as:

$$p(\mathbf{W}|\mathbf{X}, \mathbf{Y}_{\mathcal{L}}, \mathcal{G}) \propto p(\mathbf{W})p(\mathbf{Y}_{\mathcal{L}}|\mathbf{W}, \mathbf{X}, \mathcal{G}). \quad (6)$$

For predicting labels for the unlabelled nodes, we only need to draw samples from $p(\mathbf{W}|\mathbf{X}, \mathbf{Y}_{\mathcal{L}}, \mathcal{G})$, rather than explicitly evaluate the probability, so the normalization constant $1/p(\mathbf{Y}_{\mathcal{L}}|\mathbf{X}, \mathcal{G})$ can be ignored. The posterior over \mathbf{W} induces a predictive marginal posterior for the unknown node labels \mathbf{Z} as follows:

$$p(\mathbf{Z}|\mathbf{X}, \mathbf{Y}_{\mathcal{L}}, \mathcal{G}_{obs}) = \int p(\mathbf{Z}|\mathbf{W}, \mathcal{G}_{obs}, \mathbf{X})p(\mathbf{W}|\mathbf{X}, \mathbf{Y}_{\mathcal{L}}, \mathcal{G})p(\mathcal{G}|\mathcal{G}_{obs}, \mathbf{X}, \mathbf{Y}_{\mathcal{L}}) d\mathbf{W} d\mathcal{G}. \quad (7)$$

The integral in equation (7) cannot be computed in a closed form. Hence, Monte Carlo sampling is used for approximation:

$$p(\mathbf{Z}|\mathbf{X}, \mathbf{Y}_{\mathcal{L}}, \mathcal{G}_{obs}) \approx \frac{1}{N_G S} \sum_{i=1}^{N_G} \sum_{s=1}^S p(\mathbf{Z}|\mathbf{W}_{s,i}, \mathcal{G}_{obs}, \mathbf{X}). \quad (8)$$

Here, N_G graphs \mathcal{G}_i are sampled from $p(\mathcal{G}|\mathcal{G}_{obs}, \mathbf{X}, \mathbf{Y}_{\mathcal{L}})$ and subsequently for each \mathcal{G}_i , S weight matrices $\mathbf{W}_{s,i}$ are sampled from the variational approximation of $p(\mathbf{W}|\mathbf{X}, \mathbf{Y}_{\mathcal{L}}, \mathcal{G}_i)$. Due to its simplicity, we use Monte Carlo dropout [37] to generate the samples $\mathbf{W}_{s,i}$ from the variational approximation, although its generalization for GCNs in [38] could also be used.

Node copying for BGCN: The node copying model provides a way to specify $p(\mathcal{G}|\mathcal{G}_{obs}, \mathbf{X}, \mathbf{Y}_{\mathcal{L}})$ and to generate samples from it. The proposed BGCN algorithm is presented in Algorithm 1. The inputs are the observed graph, the node features and the observed labels. The outputs are soft predictions

for the unknown node labels. For the copying model, we need to specify $p(\zeta^j = m | \mathcal{G}_{obs}, \mathbf{X}, \mathbf{Y}_{\mathcal{L}})$, because this defines the graph distribution. In this setting, intuitively we believe that nodes with the *same labels* are *similar* and hence should be candidates for copying. For constructing the conditional distribution of ζ , we employ a base classification algorithm using the observed graph \mathcal{G}_{obs} , the features \mathbf{X} and the training labels $\mathbf{Y}_{\mathcal{L}}$ to obtain predictive labels $\hat{c}_\ell \in \{1, \dots, K\}$ for each node ℓ in the graph (Step 3: Initialization). Then, for each node j , we assign a uniform probability for ζ^j over all nodes with the same predictive label from the base classifier as follows:

$$p(\zeta^j = m | \mathcal{G}_{obs}, \mathbf{X}, \mathbf{Y}_{\mathcal{L}}) = \begin{cases} \frac{1}{|\mathcal{C}_k|}, & \text{if } \hat{c}_j = \hat{c}_m = k, \text{ where } \mathcal{C}_k = \{\ell \mid \hat{c}_\ell = k\} \\ 0, & \text{otherwise.} \end{cases} \quad (9)$$

In our experiments, we use the GCN [39] as a base classifier to obtain $\{\hat{c}_\ell\}$.

Algorithm 1 Bayesian GCN with node copying

- 1: **Input:** $\mathcal{G}_{obs}, \mathbf{X}, \mathbf{Y}_{\mathcal{L}}$
 - 2: **Output:** $p(\mathbf{Z} | \mathbf{X}, \mathbf{Y}_{\mathcal{L}}, \mathcal{G}_{obs})$
 - 3: **Initialization:** Train a base classifier to obtain \hat{c}_ℓ and form $\mathcal{C}_k, k = 1, 2, \dots, K$.
 - 4: **for** $i = 1$ **to** N_G **do**
 - 5: Sample graph $\mathcal{G}_i \sim p(\mathcal{G} | \mathcal{G}_{obs}, \mathbf{X}, \mathbf{Y}_{\mathcal{L}})$ from node copying model defined by (9) and (1).
 - 6: **for** $s = 1$ **to** S **do**
 - 7: Sample weights $\mathbf{W}_{s,i}$ using MC dropout by training a GCN over graph \mathcal{G}_i .
 - 8: **end for**
 - 9: **end for**
 - 10: Approximate $p(\mathbf{Z} | \mathbf{X}, \mathbf{Y}_{\mathcal{L}}, \mathcal{G}_{obs})$ using eq. (8).
-

Experiments: We evaluate node classification on standard benchmark datasets, including citation datasets Cora, Citeseer and Pubmed from [40] and Coauthor-CS from [41]. For the citation networks, we use the same hyperparameters as in [5] and for the Coauthor-CS dataset we use the largest connected component and the hyperparameters reported in [41]. We address three different scenarios, where we have access to 5, 10 or 20 labels per class. We conduct 50 trials; each trial corresponds to a random weight initialization and use of a random train/test split.

Table 2: Accuracy of semi-supervised node classification.

| Algorithms | | 5 labels | 10 labels | 20 labels | | 5 labels | 10 labels | 20 labels |
|------------|--------|------------------|------------------|------------------|----------|------------------|------------------|------------------|
| GCN | Cora | 70.0±3.7 | 76.0±2.2 | 79.8±1.8 | Citeseer | 58.5±4.7 | 65.4±2.6 | 67.8±2.3 |
| MMSBM-BGCN | | 74.6±2.8* | 77.5±2.6 | 80.2±1.5 | | 63.0±4.8 | 69.9±2.3* | 71.1±1.8* |
| DFNET-ATT | | 72.3±2.9 | 75.8 ±1.7 | 79.3±1.8 | | 60.5±1.2 | 63.2 ±2.9 | 66.3±1.7 |
| SBM-GCN | | 46.0±19 | 74.4±10 | 82.6±0.2* | | 24.5±7.3 | 43.3±12 | 66.1±5.7 |
| BGCN-Copy | | 73.8±2.7 | 77.6±2.6 | 80.3±1.6 | | 63.9±4.2* | 68.5±2.3 | 70.2±2.0 |
| GCN | Pubmed | 69.7±4.5 | 73.9±3.4 | 77.5±2.5 | Co-CS | 90.7±1.4 | 90.7±1.4 | 92.1±1.0 |
| MMSBM-BGCN | | 70.2±4.5 | 73.3±3.1 | 76.0±2.6 | | 91.0±1.0 | 91.3±1.1* | 91.6±1.0 |
| SBM-GCN | | 59.0±10 | 67.8±6.9 | 74.6±4.5 | | 88.8±1.7 | 89.8±1.7 | 91.4±1.8 |
| BGCN-Copy | | 71.0±4.2* | 74.6±3.3* | 77.5±2.4 | | 90.5±1.4 | 90.7±1.2 | 91.6±1.0 |

We compare the proposed BGCN based on node copying (BGCN-Copy) with the BGCN based on an MMSBM [33] (MMSBM-BGCN) and the SBM-GCN [34] to highlight the usefulness of the node copying model. We also include node classification baselines GCN [39] and DFNET[42] (only for Cora and Citeseer datasets due to run-time considerations). The average accuracies along with standard errors are reported in Table 2. For each setting, the highest average accuracy is written in bold and an asterisk (*) is used if the algorithm offers better performance compared to the second best algorithm that is statistically significant at the 5% level using a Wilcoxon signed rank test. (The significance test results are reported in the same way in the two following sections).

Data scarce setting: As in [34], we consider another node classification experiment where all the edges connected to the test set nodes are removed from the graph. We also have access to only 5 training examples from each class. We use a Multi Layer Perceptron (MLP) as a non-graph baseline algorithm. We conduct 20 trials for each dataset and report the average accuracies along with the standard error in Table 3.

Table 3: Accuracy of semi-supervised node classification in data-scarce setting.

| | MLP | GCN | MMSBM-BGCN | SBM-GCN | BGCN-Copy |
|--------------------|----------|----------|------------|-----------------|------------------|
| Cora | 39.7±3.7 | 53.5±3.6 | 54.7±4.6 | 25.3±12.8 | 58.7±3.5* |
| Citeseer | 40.2±3.6 | 48.3±3.3 | 47.6±2.5 | 18.1±5.4 | 54.5±2.8* |
| Pubmed | 59.2±3.4 | 66.2±4.1 | 67.1±3.9 | 57.8±7.7 | 69.1±4.0* |
| Coauthor CS | 80.5±2.5 | 85.8±2.3 | 88.2±1.2 | 88.7±1.8 | 87.4±1.6 |

Comparison of BGCN generative models with runtime analysis: Finally, we compare the node copying BGCN with BGCN variants that incorporate other graph generative models for $p(\mathcal{G}|\mathcal{G}_{obs}, \mathcal{D})$, including the generative models considered in Section 4. Performance and runtime results on the Cora dataset are reported in Table 4. Implementation details of the BGCN variants are provided in B.

Table 4: Accuracy of node classification for different size of labeled set and runtime (for a 20 labels per class trial) of various BGCNs on Cora dataset, averaged over 20 trials.

| Gen. model | VGAE | GRAPHITE | MMSBM | NETGAN | DGLFRM-B | BGCN-Copy |
|-----------------------|----------|----------|----------|-----------|-----------------|-----------------|
| 5 labels | 68.3±3.6 | 69.0±3.1 | 74.6±2.8 | 71.0±2.4 | 75.1±2.3 | 73.8±2.7 |
| 10 labels | 74.0±2.0 | 74.3±2.0 | 77.5±2.6 | 77.0±2.7 | 77.3±1.8 | 77.6±2.6 |
| 20 labels | 78.2±2.0 | 78.3±1.7 | 80.2±1.5 | 80.0±1.62 | 78.8±1.6 | 80.3±1.6 |
| Exec. time (s) | 33 | 34 | 512 | 86573 | 244 | 30 |

Discussion: From Table 2, we observe that the proposed BGCN either outperforms or offers comparable performance to the competing techniques in most cases. In the data-scarce setting, models which can incorporate the uncertainty in the graph show better performance in general as they have some capability to mitigate the effects of missing edges and fewer training labels. The proposed BGCN-Copy has the capacity of adding new edges during training, as do MMSBM-BGCN and SBM-GCN. From Table 3, we observe that the proposed algorithm shows significant improvement compared to its competitors.

Table 4 highlights that the node copying based BGCN provides much better results than VGAE or GRAPHITE and is much faster compared to the other alternatives. The proposed copying approach generalizes the BGCN to settings where the parametric model does not fit well. It also reveals that our approach is faster than MMSBM-BGCN which makes it a better alternative to process larger datasets. The parametric inference for the MMSBM is challenging for larger graphs, whereas our approach scales linearly with the number of nodes.

6 Application – Node copying for defense against adversarial attacks

We present node classification in an adversarial setting as a second application. Generally, a topological attack corrupts the prediction of a node label by tampering with its neighborhood. Since the node copying model explicitly provides new neighborhoods to nodes, we can construct a defense algorithm based on sampled graphs in which the targeted node can possibly escape the effect of the attack.

Problem Setting: We consider attacks in which unlabeled nodes $\mathcal{V}_{attacked} \subset \mathcal{L}$ are subjected to an adversarial attack that can modify the neighborhood of the targeted nodes. The defense algorithm only has access to the resulting corrupted graph $\mathcal{G}_{attacked}$, and the goal is to recover classification accuracy at the targeted nodes $v \in \mathcal{V}_{attacked}$. The complete feature matrix \mathbf{X} and the training labels

$\mathbf{Y}_{\mathcal{L}}$ of a (small) labeled set are assumed to be unperturbed. Following the categorizations of graph attacks in the survey [43], this specific adversarial setting belongs to the *edge-level, targeted, poisoning* category.

Defense algorithm using node copying: Our proposed defense procedure is summarized in Algorithm 2. We now detail the steps of the algorithm. We first train a GCN classification algorithm on the attacked graph (Step 3). Since our sole interest is in correcting the erroneous classifications at the nodes in $\mathcal{V}_{attacked}$, we do not need to sample entire graphs for this application. Instead, we sample local neighbourhoods of the targeted nodes $v \in \mathcal{V}_{attacked}$ via the node copying model $p(\zeta^v | \mathcal{G}_{attacked}, \mathbf{X})$. We note that the classifications of the attacked nodes are most likely incorrect. So, using the predicted classes to define similarities in the node copying model is not sensible as the targeted nodes might be more similar to nodes from a different class. Instead, we use an unsupervised representation of the nodes for sampling the replacement nodes. We train a node embedding algorithm using $(\mathcal{G}_{attacked}, \mathbf{X})$ to obtain the node representations $\{e_i\}_{i=1:N}$ (Step 4). A symmetric, pairwise distance matrix $D \in \mathbb{R}_+^{N \times N}$ is formed, where D_{ij} denotes a distance between e_i and e_j . (Step 5). In our experiments, we use the Graph Variational Auto Encoder (VGAE) [39] as the embedding algorithm and compute pairwise Euclidean distances to form $D : D_{i,j} = \|e_i - e_j\|_2$. For any targeted node, we sample the replacement node (Step 8) uniformly at random from the nodes which are close to the targeted node. Formally, we define:

$$p(\zeta^v = m | \mathcal{G}_{attacked}, \mathbf{X}, \mathbf{Y}_{\mathcal{L}}) = \begin{cases} \frac{1}{P}, & \text{if } D_{v,m} = D_{v,(\ell)} \text{ for some } 1 \leq \ell \leq P \\ 0, & \text{otherwise.} \end{cases} \quad (10)$$

Here $D_{i,(j)}$ is the j -th order statistic of $\{D_{i,\ell}\}_{\ell=1}^N$. For each corrupted node, our approach replaces the classification obtained from the node classifier trained on the corrupted graph $\mathcal{G}_{attacked}$ by the ensemble of classifications of the same model with the sampled ζ^v s copied in place of node v (Step 9). We use the mean of the softmax probabilities as the ensemble aggregation function (Step 11). In many graph-based models [5, 44], the node classification is primarily influenced by nodes within a few hops. As a result, a localized evaluation of the predictions at the targeted nodes can be computed efficiently.

Algorithm 2 Error correction using node copying

- 1: **Input:** $\mathcal{G}_{attacked}, \mathbf{X}, \mathbf{Y}_{\mathcal{L}}, \mathcal{V}_{attacked}$
 - 2: **Output:** $\hat{\mathbf{Y}}_{attacked}^{Copying}$
 - 3: Train a semi supervised node classification algorithm using $\mathcal{G}_{attacked}, \mathbf{X}, \mathbf{Y}_{\mathcal{L}}$ to learn model parameters \mathbf{W} .
 - 4: Train a node embedding algorithm using $\mathcal{G}_{attacked}, \mathbf{X}$ to obtain embeddings $\{e_i\}_{i=1}^N$.
 - 5: Compute the pairwise distance matrix D , where, $D_{ij} = \|e_i - e_j\|_2$.
 - 6: **for** $v \in \mathcal{V}_{attacked}$ **do**
 - 7: **for** $k = 1 : N_G$ **do**
 - 8: Sample $\zeta_k^v \sim p(\zeta^v | \mathcal{G}_{attacked}, \mathbf{X}, \mathbf{Y}_{\mathcal{L}})$ according to (10).
 - 9: Copy node ζ_k^v in place of node v and compute the prediction of the learned classifier (in Step 3) at node v , $\hat{\mathbf{y}}_v^{(\zeta_k^v)}$ using the parameters \mathbf{W} .
 - 10: **end for**
 - 11: Compute $\hat{\mathbf{y}}_v^{Copying} = \frac{1}{N_G} \sum_{k=1}^{N_G} \hat{\mathbf{y}}_v^{(\zeta_k^v)}$
 - 12: **end for**
 - 13: Form $\hat{\mathbf{Y}}_{attacked}^{Copying} = \{\hat{\mathbf{y}}_v^{Copying}\}_{v \in \mathcal{V}_{attacked}}$
-

We note that the node embeddings $\{e_i\}_{i=1}^N$ of $\mathcal{G}_{attacked}$, which are used to form $p(\zeta^v | \mathcal{G}_{attacked}, \mathbf{X}, \mathbf{Y}_{\mathcal{L}})$ are also affected by the topological attack. This can potentially degrade the effectiveness of the proposed defense mechanism. If the attack is believed to be too strong, we can use a similarity metric that ignores any topological information instead of relying on the embeddings of the nodes of the attacked graph. However, our experimental results in Table 5 demonstrates that even for a quite severe attack (where 75% of the neighbors of the targeted nodes have been tampered with), the

proposed defense strategy using node copying has impressive performance. Figure 2(b) shows how a

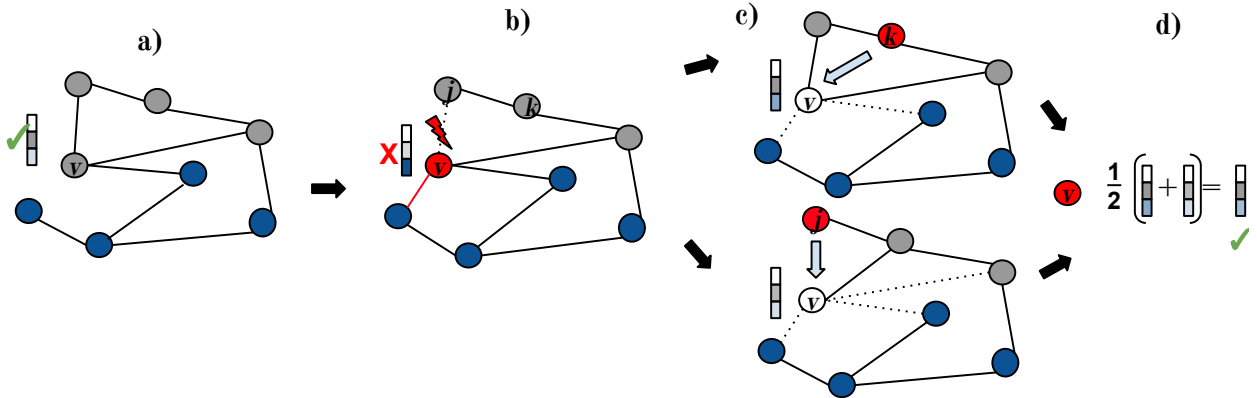


Figure 2: Summary of the node copying procedure. **a)** In the absence of the attack, the softmax of node v achieves the correct classification in \mathcal{G}_{obs} . **b)** Node v is targeted by an attack and is now wrongly classified. **c)** We sample two replacement nodes for node v : $\zeta^v = j$ and $\zeta^v = k$. The softmax vectors at node v after nodes j and k are copied in place of node v are denoted as $\hat{\mathbf{y}}_v^{(j)}$ and $\hat{\mathbf{y}}_v^{(k)}$, respectively. **d)** The error for node v is corrected by computing $\hat{\mathbf{y}}_v^{Copying} = \frac{1}{2}(\hat{\mathbf{y}}_v^{(j)} + \hat{\mathbf{y}}_v^{(k)})$.

topological attack can lead to an incorrect classification for a targeted node. Figure 2(c) provides two examples of the node copying operation to generate new graphs by copying some ζ^v s in place of node v . Figure 2(d) depicts how the softmax values derived from these generated graphs are combined to recover the original correct classification.

Experiments: Our proposed defense algorithm is evaluated against three graph adversarial attacks. *Targeted DICE* (Delete Internally Connect Externally) is the targeted version of the global attack from [45]. This algorithm attacks a node by randomly disconnecting β percent of its neighbors of the same class, and add the same number of edges to random nodes of a different class. We present results with $\beta = 50\%$ and $\beta = 75\%$. *Nettack* from [46] is another topological attack. We use the directed version of *Nettack* and set the number of perturbations to be equal to the degree of the attacked node. The last attack we consider is *FGA* [47], for which we set the number of perturbations to 20. All remaining parameters are set to the values provided in the respective papers.

In order to illustrate the effectiveness of the procedure, we compare the accuracy at the attacked nodes for the proposed copying algorithm with a standard GCN and a *state-of-the-art* defense algorithm GCN-SVD [48], for which we set the rank parameter $K = 50$. We consider a setting where \mathcal{V}_{trn} is formed with 20 labels per class. The attacked set $\mathcal{V}_{attacked}$ is simulated by randomly sampling 40 nodes, excluding \mathcal{V}_{trn} , and corrupting them with the attack.

Table 5: Accuracy of defense algorithms at the attacked node averaged over 50 trials.

| | Cora | | | | Citeseer | | | |
|----------------|------------------|------------------|----------------|----------------|------------------|-----------------|-------------------|----------------|
| | DICE 50% | DICE 75% | Nettack | FGA | DICE 50% | DICE 75% | Nettack | FGA |
| GCN | 53.4±8.9 | 31.9±8.9 | 13.6±9.6 | 69.8±16 | 45.5±7.9 | 30.45±7.6 | 11.8±5.1 | 54.6±15 |
| GCN-SVD | 51.1±9.8 | 35.9±7.1 | 41.7±11 | 57.2±15 | 48.4±7.7 | 36.3±9.1 | 34.4±8.9 * | 39.4±17 |
| Copying | 57.5±9.9* | 38.3±7.4* | 40.5±11 | 70.2±16 | 50.1±9.1* | 37.6±9.1 | 31.6±7.7 | 55.8±12 |

Discussion: From Table 5, we see that the proposed corrective mechanism based on node copying improves the classification accuracy of the corrupted nodes. Interestingly, the proposed correction procedure does not involve sampling of the entire graph or retraining of the model, rather we can perform computationally inexpensive, localized computations to improve accuracy at the targeted nodes. We observe that the GCN-SVD approach outperforms the Copying algorithm for *Nettack*, which is expected as it is tailored to provide efficient defense for this specific attack, but performs significantly worse than a standard GCN against the *FGA* attack. In contrast, the proposed Copying defense offers consistent improvement over GCN across different attacks.

7 Application – Node copying for recommender systems

As the last application, we consider the task of graph-based personalized item recommendation. An intuitive solution to this problem is to form the item recommendation of a user based on other users that have many items in common. If two users share multiple items in their interaction histories, we presume that one item purchased/liked by one of them could be recommended to the other. A node copying model can directly apply this approach by using a similarity metric between users that is proportional with the number of shared items.

Problem Setting: Let \mathcal{U} be the set of users and \mathcal{I} be the set of items. \mathcal{G}_{obs} is the partially observed bipartite graph built from previous user-item interactions. The task is to infer other unobserved interactions, which can be seen as a link prediction problem [49, 50]. Alternatively, we can view this task as a ranking problem [51]. For each user u , for an observed interaction with item i and a non-observed interaction with item j , we have $i >_u j$ in the training set. If both (u, i) and (u, j) are observed, we do not have a ranking. Using this interaction data $\{>_u\}_{trn} = \{(u, i, j) : (u, i) \in \mathcal{G}_{obs}, (u, j) \notin \mathcal{G}_{obs}\}$ for fitting a model, the task is to rank all (u, i, j) such that both (u, i) and $(u, j) \notin \mathcal{G}_{obs}$. The sets of pairs $\{(u, i) : (u, i) \in \mathcal{G}_{obs}\}$ and $\{(u, j) : (u, j) \notin \mathcal{G}_{obs}\}$ are referred to as the positive and negative pools of interactions respectively. We denote the test set as $\{>_u\}_{test} = \{(u, i, j) : (u, i) \notin \mathcal{G}_{obs}, (u, j) \notin \mathcal{G}_{obs}\}$. We consider a Bayesian Personalized Recommendation (BPR) framework [51] (details in C) along with the inference of the graph \mathcal{G} .

Background: Many existing graph-based deep learning recommender system models [52, 49, 50] learn weights \mathbf{W} to form an embedding $e_u(\mathbf{W}, \mathcal{G}_{obs})$ for the u -th user and $e_i(\mathbf{W}, \mathcal{G}_{obs})$ for the i -th item node. The ranking of any (u, i, j) triple such that both $(u, i) \notin \mathcal{G}_{obs}$ and $(u, j) \notin \mathcal{G}_{obs}$ is specified as $p(i >_u j | \mathcal{G}_{obs}, \mathbf{W}) = \sigma(e_u \cdot e_i - e_u \cdot e_j)$, where $\sigma(\cdot)$ is the sigmoid function and \cdot denotes the inner product. Assuming a suitable prior on \mathbf{W} , the learning goal is to maximize the posterior of \mathbf{W} on the training set. Here, $\widehat{\mathbf{W}} = \arg \max_{\mathbf{W}} p(\mathbf{W} | \{>_u\}_{trn}, \mathcal{G}_{obs})$ is learned by maximizing the BPR objective using Stochastic Gradient Descent (SGD). The pairwise ranking probabilities in the test set is then computed using $\widehat{\mathbf{W}}$.

Ensemble BPR: We summarize the proposed Ensemble BPR algorithm in Algorithm 3. For the Ensemble BPR algorithm, we first obtain $\widehat{\mathbf{W}}$ as previously described (Step 3), then we evaluate the ranking by computing an expectation with respect to the random graph \mathcal{G} , sampled from the node copying model.

Algorithm 3 Ensemble BPR with node copying

- 1: **Input:** $\mathcal{G}_{obs}, \{>_u\}_{trn}$
 - 2: **Output:** $p(\{>_u\}_{test} | \{>_u\}_{trn}, \mathcal{G}_{obs})$
 - 3: Obtain $\widehat{\mathbf{W}} = \arg \max_{\mathbf{W}} p(\mathbf{W} | \{>_u\}_{trn}, \mathcal{G}_{obs})$ by minimizing the BPR loss.
 - 4: **for** $i = 1$ **to** N_G **do**
 - 5: Sample graph $\mathcal{G}_i \sim p(\mathcal{G} | \mathcal{G}_{obs}, \{>_u\}_{trn})$ using the node copying model defined by (11).
 - 6: **end for**
 - 7: Approximate $p(\{>_u\}_{test} | \{>_u\}_{trn}, \mathcal{G}_{obs})$ using eq. (13).
-

In this setting, we assign a non-zero conditional probability to only the class of bipartite graphs since \mathcal{G}_{obs} is bipartite. This is achieved by considering a node copying scheme where only user nodes can be copied to a user node. We consider that users that share items are similar, so we use the Jaccard index ρ between the sets of items for pairs of users to define the conditional probability distribution of ζ as follows:

$$p(\zeta^j = m | \mathcal{G}_{obs}) = \begin{cases} \rho(j, m) / \sum_{i \in \mathcal{U}} \rho(j, i), & \text{if } j, m \in \mathcal{U} \\ 0, & \text{otherwise} \end{cases} \quad (11)$$

We compute the pairwise ranking probabilities in the test set as follows:

$$p(\{>_u\}_{test}|\{>_u\}_{trn}, \mathcal{G}_{obs}) = \int p(\{>_u\}_{test}|\mathcal{G}, \mathbf{W})p(\mathbf{W}|\{>_u\}_{trn}, \mathcal{G}_{obs})p(\mathcal{G}|\mathcal{G}_{obs}, \{>_u\}_{trn})d\mathbf{W}d\mathcal{G}. \quad (12)$$

We sample N_G graphs \mathcal{G}_i s from $p(\mathcal{G}|\mathcal{G}_{obs}, \{>_u\}_{trn})$ using node copying (Step 5) and then form a Monte Carlo approximation of eq. (12) as follows (Step 7):

$$p(\{>_u\}_{test}|\{>_u\}_{trn}, \mathcal{G}_{obs}) \approx \frac{1}{N_G} \sum_{i=1}^{N_G} p(\{>_u\}_{test}|\mathcal{G}_i, \widehat{\mathbf{W}}), \quad (13)$$

Implementation of eq. (13) does not require retraining of the model since $\widehat{\mathbf{W}}$ is already obtained by minimizing the BPR loss; it only involves evaluation of a trained model on multiple sampled graphs to compute the average pairwise ranking probability for the test set.

Sampled Graph BPR (SGBPR) — training with sampled graphs:

We consider another approach where we use the generated graphs during the training process as well. The SGBPR algorithm is summarized in Algorithm 4.

Algorithm 4 Sampled Graph BPR with node copying

- 1: **Input:** $\mathcal{G}_{obs}, \{>_u\}_{trn}$
 - 2: **Output:** $p(\{>_u\}_{test}|\{>_u\}_{trn}, \mathcal{G}_{obs})$
 - 3: **for** $i = 1$ **to** N_G **do**
 - 4: Sample graph $\mathcal{G}_i \sim p(\mathcal{G}|\mathcal{G}_{obs}, \{>_u\}_{trn})$ using the node copying model defined by (11).
 - 5: **end for**
 - 6: Compute $\widehat{A}_{\widehat{\mathcal{G}}}$ using eq. (15) and $\widehat{\mathcal{G}}_b$ (equivalently $A_{\widehat{\mathcal{G}}_b}$) using $\widehat{A}_{\widehat{\mathcal{G}}}$.
 - 7: Compute $f(\widehat{\mathcal{G}}_{obs}) = \mathcal{G}_{obs} \cup \widehat{\mathcal{G}}_b$
 - 8: Obtain $\widehat{\mathbf{W}}' = \arg \max_{\mathbf{W}} p(\mathbf{W}|\{>_u\}_{trn}, \mathcal{G}_{obs}, f(\widehat{\mathcal{G}}_{obs}))$ by minimizing the BPR loss.
 - 9: Approximate $p(\{>_u\}_{test}|\{>_u\}_{trn}, \mathcal{G}_{obs})$ using eq. (16).
-

Our motivation is to remove some of the potentially unobserved positive interactions in the training set from the negative interaction pool. We rely on the node copying model to sample graphs (Step 4), which potentially contain positive interactions between user-item pairs, which are unobserved in \mathcal{G}_{obs} . The inference of graph \mathcal{G} is carried out from the copying model $p(\mathcal{G}|\mathcal{G}_{obs}, \{>_u\}_{trn})$ specified in eq. (11). We need to compute:

$$p(\{>_u\}_{test}|\{>_u\}_{trn}, \mathcal{G}_{obs}) = \int p(\{>_u\}_{test}|\mathcal{G}, \mathbf{W})p(\mathbf{W}|\{>_u\}_{trn}, \mathcal{G}_{obs}, f(\mathcal{G}_{obs}))p(\mathcal{G}|\mathcal{G}_{obs}, \{>_u\}_{trn})d\mathbf{W}d\mathcal{G}. \quad (14)$$

Here, $f(\mathcal{G}_{obs})$ is a function of the observed graph that returns a graph that is used to control the negative pool. There is flexibility in the choice of this function, but we use $f(\mathcal{G}_{obs}) = \mathcal{G}_{obs} \cup \overline{\mathcal{G}}_b$. The union \cup indicates that we take the union of the edge sets of the two graphs. We define $\overline{\mathcal{G}} \triangleq \mathbb{E}_{\mathcal{G}|\mathcal{G}_{obs}}[\mathcal{G}]$ as the graph with adjacency matrix equal to the expectation of the adjacency matrix over the generative graph distribution. The graph $\overline{\mathcal{G}}_b$ is derived from this; it has a binary adjacency matrix derived by comparing the adjacency matrix entries of $\overline{\mathcal{G}}$ to a small positive threshold b . So, we have $A_{\overline{\mathcal{G}}_b} = \mathbb{1}[A_{\overline{\mathcal{G}}} > b]$. Due to analytical intractability, we approximate $\mathbb{E}_{\mathcal{G}|\mathcal{G}_{obs}}[\mathcal{G}]$ using Monte Carlo. This amounts to approximating the adjacency matrix of $\overline{\mathcal{G}} = \mathbb{E}_{\mathcal{G}|\mathcal{G}_{obs}}[\mathcal{G}]$, whose (s, w) -th entry can be estimated as:

$$\widehat{A}_{\overline{\mathcal{G}}}(s, w) = \frac{1}{N_G} \sum_{i=1}^{N_G} A_{\mathcal{G}_i}(s, w). \quad (15)$$

Here, $\mathcal{G}_i \sim p(\mathcal{G}|\mathcal{G}_{obs}, \{>_u\}_{trn})$ is sampled from the node copying model in Step 4. This allows us to construct an estimate $f(\widehat{\mathcal{G}}_{obs})$ by first computing an approximate $\widehat{\mathcal{G}}_b$ (equivalently $A_{\widehat{\mathcal{G}}_b}$) using $\widehat{A}_{\widehat{\mathcal{G}}}$ (Step 6) and then using this $\widehat{\mathcal{G}}_b$ in the definition of $f(\mathcal{G}_{obs})$ (Step 7).

In specifying $p(\mathbf{W}|\{\>_u\}_{trn}, \mathcal{G}_{obs}, f(\mathcal{G}_{obs}))$, we effectively aim to reduce the training set by eliminating unobserved edges from the negative pool. We have $\{\>_u\}_{trn} = D_S$. We now introduce $D'_S = D_S \setminus \{(u, i, j) : (u, i) \in \mathcal{G}_{obs}, (u, j) \in \overline{\mathcal{G}}_b\}$, and set $p(\mathbf{W}|\{\>_u\}_{trn}, \mathcal{G}_{obs}, f(\mathcal{G}_{obs})) = p(\mathbf{W}|D'_S)$, which amounts to training the model based on positive and negative interactions in D'_S . Using $\widehat{\mathbf{W}}' = \arg \max_{\mathbf{W}} p(\mathbf{W}|\{\>_u\}_{trn}, \mathcal{G}_{obs}, f(\widehat{\mathcal{G}}_{obs}))$ (Step 8), the posterior probability of $\{\>_u\}_{test}$ in eq. (14) is then approximated as:

$$p(\{\>_u\}_{test}|\{\>_u\}_{trn}, \mathcal{G}_{obs}) \approx \frac{1}{N_G} \sum_{i=1}^{N_G} p(\{\>_u\}_{test}|\mathcal{G}_i, \widehat{\mathbf{W}}') \quad (16)$$

Experiments: For the recommender system, we use two datasets (ML100k and Amazon-CDs, with details in Table 8 in A) that we preprocess by retaining users and items that have a specified minimum number of edges set by a threshold. We create training, validation and test sets by splitting the data 70/10/20%. We generate random splits for each of the 10 trials and report average Recall and Normalized Discounted Cumulative Gain (NDCG) at 10 and 20. *Recall@k* measures the proportion of the true (preferred) items from the top- k recommendation. For a user $u \in \mathcal{U}$, the algorithm recommends an ordered set (in descending order of preference) of top- k items $I_k(u) = \{i_n\}_{n=1}^k \subset \mathcal{I}$. There is a set of true preferred items for a user \mathcal{I}_u^+ and the number of true positive is $|\mathcal{I}_u^+ \cap I_k(u)|$, so the recall is computed as follows: $\text{Recall}@k = \frac{|\mathcal{I}_u^+ \cap I_k(u)|}{|I_k(u)|}$. Normalized Discounted Cumulative Gain (NDCG) [53] computes a score for recommendation $I_k(u)$ which emphasizes higher-ranked true positives. $D_k(n) = \mathbb{1}[i_n \in \mathcal{I}_u^+]/\log_2(n+1)$ accounts for a relevancy score. $\text{NDCG}@k = \frac{\text{DCG}_k}{\text{IDCG}_k} = \frac{\sum_{i_n \in I_k(u)} D_k(n)}{\sum_{i_n \in \mathcal{I}_{u,k}^+} D_k(n)}$, where $\mathcal{I}_{u,k}^+$ is the ordered set of top- k true preferred items in descending order of preference. We use the embedding model (MGCCF) presented in [54], which achieves *state-of-the-art* performance for this task.

Table 6: Average recall and NDCG for recommender system experiment.

| | MGCCF | EBPR | SGBPR | | MGCCF | EBPR | SGBPR |
|------------------|------------|-------------|--------------------|----------|------------|-------------|--------------------|
| Recall@10 | 19.91±0.20 | 20.15±0.07* | 20.96±0.23* | Ana.-CDs | 13.28±0.05 | 13.21±0.01* | 13.83±0.19* |
| Recall@20 | 31.27±0.21 | 31.56±0.07* | 32.45±0.34* | | 20.26±0.05 | 20.37±0.02* | 20.95±0.22* |
| NDCG@10 | 26.50±0.20 | 26.86±0.07* | 27.66±0.24* | | 14.86±0.04 | 14.78±0.01* | 15.31±0.20* |
| NDCG@20 | 31.90±0.14 | 32.23±0.06* | 33.14±0.31* | | 18.63±0.04 | 18.65±0.02 | 19.20±0.20* |

Discussion: From Table 6, we observe that for the recommendation task, adaptation of the copying model results in a simple intuitive ‘EBPR’ algorithm which improves recall over the baseline and does not involve any retraining. Use of the sampled graphs to train the model offers significantly better performance.

8 Conclusion

We present a novel generative model for graphs called node copying. The proposed model is based on the idea that neighbourhoods of similar nodes in a graph are similar and can be swapped. It is flexible and can incorporate many existing graph-based learning techniques for identifying node similarity. Sampling of graphs from this model is simple. The sampled graphs preserve important structural properties. We have demonstrated that the use of the model can improve performance for a variety of downstream learning tasks. Future work will investigate developing more general measures of similarity among the nodes of a graph and incorporating them in the copying model, and exploring potential extensions of our theoretical results to more general graphon models.

A Description of the datasets

Table 7: Statistics of evaluation datasets for node classification and generative graph models.

| Dataset | Cora | Citeseer | Pubmed | Coauthor CS | Amazon-Photo | Bitcoin | Polblogs |
|---------------------|-------|----------|--------|-------------|--------------|---------|----------|
| No. Classes | 7 | 6 | 3 | 15 | 8 | 2 | 2 |
| No. Features | 1,433 | 3,703 | 500 | 6805 | 745 | 166 | N/A |
| No. Nodes | 2,485 | 2110 | 19,717 | 18,333 | 7,487 | 472 | 1222 |
| Edge Density | 0.04% | 0.04% | 0.01% | 0.01% | 0.11% | 0.11% | 0.56% |

Table 8: Statistics of evaluation datasets for the recommender system experiments.

| Dataset | Threshold | # Users | # Items | # Interactions | Density |
|-------------------|-----------|---------|---------|----------------|---------|
| ML100k | 10 | 897 | 823 | 52,857 | 7.15% |
| Amazon-CDs | 30 | 5,479 | 2,605 | 137,313 | 0.96% |

We conduct experiments on seven datasets. In the citation datasets (Cora [40], Citeseer [40], and Pubmed [55]), nodes represent research papers and the task is to classify them into topics. The graph is built by adding an undirected edge when one paper cites another and features are derived from the keywords of the document. Coauthor CS is a coauthorship graph where each node is an author and two authors are connected if they have coauthored a paper. The node features represent keywords from each author’s papers and the node labels are the active area of research of the authors. Amazon-Photo [41] is a portion of the Amazon co-purchase dataset graph from [56]. In this case nodes are products, the features are based on the reviews, and the label is the product type. Items often bought together are linked in the graph. The bitcoin dataset is a transactional network snapshot taken from the dynamic graphs provided in the Elliptic Bitcoin Dataset [57]. In this dataset, nodes represent transactions and edges represent a directed bitcoin flow. Each transaction is labeled as being either fraudulent or legitimate. Polblogs [58] dataset is a political blogs network.

B Details of the generative models used for BGCN

For the node classification experiments comparing different candidate generative models, we use the following hyperparameters and test settings. All of the choices are inherited from the respective original papers. For VGAE [5] and GRAPHITE [24], we use a two layer GCN with 32 dimensional hidden layer and 16 dimensional encoding. The model is trained for 200 epochs with learning rate 0.01. In DGLFRM-B [7], we set $\alpha = 50$ and $K = 100$.

The encoder network has two nonlinear GCN layers with dimensions 64 and 100. The decoder network has two layers with dimension 32 and 16. The model is trained for 1000 epochs with a learning rate of 0.01 and dropout rate 0.5. All models are trained on 100% of the dataset (no test edges are held out, because the task of interest is not link prediction). For the MMSBM, we use the same settings that are reported in [59]: $\eta = 1, \alpha = 1, \rho = 0.001$. The mini-batch size for SGD is $n = 500$ and the hyperparameters related to the decaying step size are $\epsilon_0 = 1, \tau = 1024$ and $\kappa = 0.5$. For the NETGAN, we set the stopping parameter EO at 50% using a validation set of 15% of the links. Due to computation limitations, we used random walks of 10K steps to generate the graphs. The remaining hyperparameters are set to the values reported in [8]: the generator and the discriminator are respectively set to 40 and 30 layers. The noise is generated by a 16-dimensional multivariate Gaussian distribution. We use the Adam optimizer with a learning rate of 0.0003 with $\lambda_{L_2} = 10^{-6}$. The length of the random walks is set to 16. For more details, the complete list of hyperparameters can be found in section H of the supplementary material of [8].

C BPR for recommendation

In [51], Rendle et al. introduce Bayesian Personalized Ranking (BPR) framework for recommendation systems. Following the notations in Section 7, we denote the set of items that are neighbours in the observed graph for user u as $\mathcal{I}_u^+ := \{i \in \mathcal{I} : (u, i) \in \mathcal{G}_{obs}\}$. The training set can then be written as $D_S := \{(u, i, j) | i \in \mathcal{I}_u^+ \wedge j \in \mathcal{I} \setminus \mathcal{I}_u^+\}$.

In other words, the training set is all triples (u, i, j) such that user u interacted with i but did not interact with j . The test set, denoted \bar{D}_S comprises all triples (u, i, j) such that neither edge (u, i) nor (u, j) appears in \mathcal{G}_{obs} . The goal of the recommender system is to generate a total ranking $>_u$ of all items for each user u . The relation $i >_u j$ specifies that user u prefers item i to item j .

In the Bayesian personalized ranking framework of [51], our task is to maximize: $p(\Theta | \{>_u\}_{D_S}) \propto p(\{>_u\}_{D_S} | \Theta) p(\Theta)$. Here Θ are the parameters of the model, and $\{>_u\}_{D_S}$ are the observed preferences in the training data. We aim to identify the parameters Θ that maximize this posterior over all users and all pairs of items. If users are assumed to act independently, then we can write:

$$p(\{>_u\}_{D_S} | \Theta) = \prod_{(u,i,j) \in D_S} p(i >_u j | \Theta) \quad (17)$$

We define the probability that a user prefers item i over j as $p(i >_u j | \Theta) := \sigma(\hat{x}_{uij}(\Theta))$. Here \hat{x}_{uij} is a function of the model parameters Θ and the observed graph for each triple (u, i, j) . In our case, we use the difference between the dot products of the user and item embeddings, so $\hat{x}_{uij}(\Theta) = e_u(\Theta) \cdot e_i(\Theta) - e_u(\Theta) \cdot e_j(\Theta)$. If we adopt a normal distribution as the prior for $p(\Theta)$ then we can formulate the optimization objective as:

$$\text{BPR-OPT} := \ln p(\Theta | \{>_u\}_{D_S}) = \sum_{(u,i,j) \in D_S} \ln \sigma(\hat{x}_{uij}) - \lambda_{\Theta} \|\Theta\|^2 \quad (18)$$

We maximize this via stochastic gradient descent by repeatedly drawing triples (u, i, j) randomly from the training set and updating the model parameters Θ .

References

- [1] A. Goldenberg, A. X. Zheng, S. E. Fienberg, and E. M. Airoldi, “A survey of statistical network models,” *Found. Trends Mach. Learn.*, vol. 2, no. 2, p. 129–233, 2010.
- [2] R. Albert and A. L. Barabási, “Statistical mechanics of complex networks,” *Rev. Modern Physics*, vol. 74, no. 1, p. 47–97, 2002.
- [3] P. Erdős and A. Rényi, “On random graphs I,” *Publicationes Mathematicae Debrecen*, vol. 6, p. 290, 1959.
- [4] E. M. Airoldi, D. M. Blei, S. E. Fienberg, and E. P. Xing, “Mixed membership stochastic block-models,” in *Proc. Adv. Neural Info. Process. Syst.*, 2009, pp. 33–40.
- [5] T. Kipf and M. Welling, “Variational graph auto-encoders,” in *Proc. Bayesian Deep Learning Workshop, Adv. Neural Info. Process. Syst.*, 2016.
- [6] A. Grover and J. Leskovec, “node2vec: Scalable feature learning for networks,” in *Proc. ACM Int. Conf. Knowl. Disc. Data Mining*, 2016.
- [7] N. Mehta, L. C. Duke, and P. Rai, “Stochastic blockmodels meet graph neural networks,” in *Proc. Int. Conf. Machine Learning*, 2019, pp. 4466–4474.
- [8] A. Bojchevski, O. Shchur, D. Zügner, and S. Günnemann, “NetGAN: Generating graphs via random walks,” in *Proc. Int. Conf. Machine Learning*, 2018, pp. 609–618.

- [9] H. Wang, J. Wang, J. Wang, M. Zhao, W. Zhang, F. Zhang, X. Xie, and M. Guo, “GraphGAN: graph representation learning with generative adversarial nets,” in *Proc. AAAI Conf. Artificial Intell.*, 2017, pp. 2508–2515.
- [10] J. Zhu, Y. Yan, L. Zhao, M. Heimann, L. Akoglu, and D. Koutra, “Beyond homophily in graph neural networks: Current limitations and effective designs,” in *Proc. Adv. Neural Info. Process. Syst.*, 2020, pp. 7793–7804.
- [11] S. Pal, F. Regol, and M. Coates, “Bayesian graph convolutional neural networks using node copying,” in *Proc. Learning and Reasoning with Graph-Structured Representations Workshop, Int. Conf. Machine Learning*, 2019.
- [12] F. Regol, S. Pal, and M. Coates, “Node copying for protection against graph neural network topology attacks,” in *Proc. IEEE Int. Conf. Comput. Adv. Multi-Sensor Adaptive Process.*, 2019.
- [13] F. Caron and E. B. Fox, “Sparse graphs using exchangeable random measures,” *J. Royal Statistical Society: Series B (Statist. Method.)*, vol. 79, no. 5, pp. 1295–1366, 2017.
- [14] K. Nowicki and T. A. B. Snijders, “Estimation and prediction for stochastic blockstructures,” *J. American Statistical Association*, vol. 96, no. 455, pp. 1077–1087, 2001.
- [15] L. Peng and L. Carvalho, “Bayesian degree-corrected stochastic blockmodels for community detection,” *Electron. J. Statist.*, vol. 10, no. 2, pp. 2746–2779, 2016.
- [16] P. Latouche, E. Birmelé, and C. Ambroise, “Overlapping stochastic block models with application to the french political blogosphere,” *Annals Applied Statist.*, vol. 5, no. 1, pp. 309 – 336, 2011.
- [17] K. T. Miller, T. L. Griffiths, and M. I. Jordan, “Nonparametric latent feature models for link prediction,” in *Proc. Adv. Neural Info. Process. Syst.*, 2009, pp. 1276–1284.
- [18] B. Fosdick, D. Larremore, J. Nishimura, and J. Ugander, “Configuring random graph models with fixed degree sequences,” *SIAM Review*, vol. 60, no. 2, pp. 315–355, 2018.
- [19] G. Casiraghi, “Analytical formulation of the block-constrained configuration model,” *arXiv preprint: arXiv 1811.05337*, 2018.
- [20] M. Drobyshevskiy and D. Turdakov, “Random graph modeling: A survey of the concepts,” *ACM Comput. Surv.*, vol. 52, no. 6, pp. 1–36, 2019.
- [21] K. Bringmann, R. Keusch, and J. Lengler, “Geometric inhomogeneous random graphs,” *Theoretical Comput. Science*, vol. 760, pp. 35–54, 2019.
- [22] V. Veitch and D. M. Roy, “The class of random graphs arising from exchangeable random measures,” *arXiv preprint: arXiv 1512.03099*, 2015.
- [23] S. Pan, R. Hu, G. Long, J. Jiang, L. Yao, and C. Zhang, “Adversarially regularized graph autoencoder for graph embedding,” in *Proc. Int. Joint Conf. on Artificial Intell.*, 2018, pp. 2609–2615.
- [24] A. Grover, A. Zweig, and S. Ermon, “Graphite: Iterative generative modeling of graphs,” in *Proc. Int. Conf. Machine Learning*, 2019, pp. 2434–2444.
- [25] M. Simonovsky and N. Komodakis, “GraphVAE: Towards generation of small graphs using variational autoencoders,” in *Proc. Int. Conf. Artificial Neural Networks and Machine Learning*, 2018, pp. 412–422.
- [26] T. Ma, J. Chen, and C. Xiao, “Constrained generation of semantically valid graphs via regularizing variational autoencoders,” in *Proc. Adv. Neural Info. Process. Syst.*, 2018, pp. 7113–7124.

- [27] N. De Cao and T. Kipf, “MolGAN: An implicit generative model for small molecular graphs,” in *Proc. Workshop on Theoretical Foundations and Applications of Deep Generative Models, Int. Conf. Machine Learning*, 2018.
- [28] Y. Li, O. Vinyals, C. Dyer, R. Pascanu, and P. Battaglia, “Learning deep generative models of graphs,” *arXiv preprint: arXiv 1803.03324*, 2018.
- [29] J. You, R. Ying, X. Ren, W. Hamilton, and J. Leskovec, “GraphRNN: Generating realistic graphs with deep auto-regressive models,” in *Proc. Int. Conf. Machine Learning*, 2018, pp. 5708–5717.
- [30] R. Liao, Y. Li, Y. Song, S. Wang, C. Nash, W. Hamilton, D. K. Duvenaud, R. Urtasun, and R. Zemel, “Efficient graph generation with graph recurrent attention networks,” in *Proc. Adv. Neural Info. Process. Syst.*, 2019, pp. 4257–4267.
- [31] X. Dong, D. Thanou, P. Frossard, and P. Vandergheynst, “Learning laplacian matrix in smooth graph signal representations,” *IEEE Trans. Sig. Proc.*, vol. 64, no. 23, pp. 6160–6173, 2016.
- [32] V. Kalofolias and N. Perraudin, “Large Scale Graph Learning from Smooth Signals,” in *Proc. Int. Conf. Learning Representations*, 2019.
- [33] Y. Zhang, S. Pal, M. Coates, and D. Üstebay, “Bayesian graph convolutional neural networks for semi-supervised classification,” in *Proc. AAAI Conf. Artificial Intell.*, 2019, pp. 5829–5836.
- [34] J. Ma, W. Tang, J. Zhu, and Q. Mei, “A flexible generative framework for graph-based semi-supervised learning,” in *Proc. Adv. Neural Info. Process. Syst.*, 2019, pp. 3276–3285.
- [35] P. Elinas, E. V. Bonilla, and L. Tiao, “Variational inference for graph convolutional networks in the absence of graph data and adversarial settings,” in *Proc. Adv. Neural Info. Process. Syst.*, 2020, pp. 18 648–18 660.
- [36] S. Pal, S. Malekmohammadi, F. Regol, Y. Zhang, Y. Xu, and M. Coates, “Non-parametric graph learning for Bayesian graph neural networks,” in *Proc. Conf. Uncertainty Artificial Intell.*, 2020, pp. 1318–1327.
- [37] Y. Gal and Z. Ghahramani, “Dropout as a Bayesian approximation: Representing model uncertainty in deep learning,” in *Proc. Int. Conf. Machine Learning*, 2016, pp. 1050–1059.
- [38] A. Hasanzadeh, E. Hajiramezanali, S. Boluki, M. Zhou, N. Duffield, K. Narayanan, and X. Qian, “Bayesian graph neural networks with adaptive connection sampling,” in *Proc. Int. Conf. Machine Learning*, 2020, pp. 4094–4104.
- [39] T. Kipf and M. Welling, “Semi-supervised classification with graph convolutional networks,” in *Proc. Int. Conf. Learning Representations*, 2017.
- [40] P. Sen, G. Namata *et al.*, “Collective classification in network data,” *AI Magazine*, vol. 29, no. 3, pp. 93–106, 2008.
- [41] O. Shchur, M. Mumme, A. Bojchevski, and S. Günnemann, “Pitfalls of graph neural network evaluation,” in *Proc. Relational Representation Learning Workshop, Adv. Neural Info. Process. Syst.*, 2018.
- [42] A. Wijesinghe and Q. Wang, “DFNets: Spectral CNNs for graphs with feedback-looped filters,” in *Proc. Adv. Neural Info. Process. Syst.*, 2019, pp. 6007–6018.
- [43] L. Sun, J. Wang, P. S. Yu, and B. Li, “Adversarial attack and defense on graph data: a survey,” *arXiv preprint: arXiv 1812.10528*, 2018.
- [44] P. Veličković, G. Cucurull, A. Casanova, A. Romero, P. Liò, and Y. Bengio, “Graph attention networks,” in *Proc. Int. Conf. Learning Representations*, 2018.

- [45] M. Waniek, T. P. Michalak, M. J. Wooldridge, and T. Rahwan, “Hiding individuals and communities in a social network,” *Nature Human Behaviour*, vol. 2, no. 2, pp. 139–147, 2018.
- [46] D. Zügner, A. Akbarnejad, and S. Günnemann, “Adversarial attacks on neural networks for graph data,” in *Proc. Int. Conf. on Knowledge Discovery & Data Mining*, 2018, pp. 2847–2856.
- [47] J. Chen, Y. Wu, X. Xu, Y. Chen, H. Zheng, and Q. Xuan, “Fast gradient attack on network embedding,” *arXiv preprint: arXiv 1809.02797*, 2018.
- [48] N. Entezari, S. A. Al-Sayouri, A. Darvishzadeh, and E. E. Papalexakis, “All you need is low rank: defending against adversarial attacks on graphs,” in *Proc. Int. Conf. on Web Search and Data Mining*, 2020, pp. 169–177.
- [49] X. Wang, X. He, M. Wang, F. Feng, and T. Chua, “Neural graph collaborative filtering,” in *Proc. Conf. Research and Development in Info. Retrieval*, 2019, pp. 165–174.
- [50] R. Ying, R. He, K. Chen, P. Eksombatchai, W. L. Hamilton, and J. Leskovec, “Graph convolutional neural networks for web-scale recommender systems,” in *Proc. Int. Conf. on Knowledge Discovery & Data Mining*, 2018, pp. 974–983.
- [51] S. Rendle, C. Freudenthaler, Z. Gantner, and L. Schmidt-Thieme, “BPR: Bayesian personalized ranking from implicit feedback,” in *Proc. Conf. Uncertainty in Artificial Intell.*, 2009, pp. 452–461.
- [52] J. Sun, Y. Zhang, C. Ma, M. Coates, H. Guo, R. Tang, and X. He, “Multi-graph convolution collaborative filtering,” in *Proc. IEEE Int. Conf. on Data Mining*, 2019, pp. 1306–1311.
- [53] K. Järvelin and J. Kekäläinen, “IR evaluation methods for retrieving highly relevant documents,” in *Proc. Int. ACM SIGIR Conf. Research and Development in Inf. Retrieval*, 2000, pp. 41–48.
- [54] K. Sun, P. Koniusz, and J. Wang, “Fisher-Bures adversary graph convolutional networks,” in *Proc. Conf. Uncertainty in Artificial Intell.*, 2019.
- [55] G. Namata, B. London, L. Getoor, and B. Huang, “Query-driven active surveying for collective classification,” in *Proc. Workshop on Mining and Learning with Graphs, Int. Conf. Machine Learning*, 2012.
- [56] J. McAuley, C. Targett, Q. Shi, and A. van den Hengel, “Image-based recommendations on styles and substitutes,” in *Proc. Int. ACM SIGIR Conf. Research and Development Info. Retrieval*, 2015, pp. 43–52.
- [57] M. Weber, G. Domeniconi, J. Chen, D. K. I. Weidele, C. Bellei, T. Robinson, and C. E. Leiserson, “Anti-money laundering in bitcoin: Experimenting with graph convolutional networks for financial forensics,” in *Proc. KDD Deep Learning on Graphs: Methods and Applications workshop*, 2018.
- [58] L. A. Adamic and N. Glance, “The political blogosphere and the 2004 U.S. election: Divided they blog,” in *Proc. Int. Workshop on Link Discovery*, 2005, pp. 36–43.
- [59] X. Zhang, C. Moore, and M. Newman, “Random graph models for dynamic networks,” *Eur. Phys. J. B*, pp. 90–200, 2017.